RSC Advances

ROYAL SOCIETY OF CHEMISTRY

www.rsc.org/advances

Journal Name

ARTICLE

Reducing the cytotoxicity of ZnO nanoparticles by pre-formed protein corona in supplemented cell culture medium

Received 00th January 20xx,
Accepted 00th January 20xx

DOI: 10.1039/x0xx00000x

www.rsc.org/

Hong Yin,[†*ab] Rui Chen,[†c] Philip S Casey,[a] Pu Chun Ke,[b] Thomas P Davis[bd] and Chunying Chen[c]

The safety of zinc oxide (ZnO) nanoparticles (NPs) remains a critical concern considering that they are a common constituent in cosmetics and sunscreen formulation. In our study, the cytotoxicity of pristine ZnO NPs in human hepatocellular carcinoma (HepG2) cell line was found to be significantly reduced when the NPs were pre-incubated in supplemented cell culture medium for 24 h prior to actual cell exposure. These pre-coated particles developed a stable protein layer on their surfaces, which facilitated further protein adsorption during the cell culture process. The amount of proteins adsorbed on pre-coated NPs was significantly larger and the affinity between the NPs and proteins was stronger, which inhibited both ROS generation and ZnO dissolution and resulted in lower cytotoxicity compared to pristine NPs. Our studies on the continued evolution of hard protein corona on ZnO NPs in supplemented cell culture medium and its effects on cytotoxicity demonstrate an effective and convenient way to achieve safe biomedical and environmental applications of ZnO NPs and may be extrapolated to other classes of engineered nanomaterials.

Introduction

Nanoparticles (NPs) are increasingly being utilized in a variety of fields such as catalysis, gas sensing, electronics, and environmental remediation, and are integrated into commercial products and biomedical applications due to their unique physicochemical characteristics. Zinc oxide (ZnO) NPs, for example, are a common constituent of personal care products including cosmetics and sunscreens, because they efficiently absorb ultraviolet radiation and are also highly transparent to visible light. Submicrometer- and micrometer-sized ZnO particles, however, do not possess this combination of advantageous properties.[1] Some recent studies have shown that ZnO NPs can be toxic to a wide variety of biological systems, including epidermal cells,[2] bacteria (*Streptococcus agalactiae* and *Staphylococcus aureus*),[3] zebra fish (*Danio rerio*),[4] and mice.[5] Moreover, ZnO was more toxic to *Escherichia coli* than other metal oxide NPs such as Fe_2O_3, Y_2O_3, TiO_2, and CuO.[6] Surface modification of ZnO NPs has been proved to be an effective strategy in mitigating the toxicity of the NPs. For example, coating ZnO surface with a silica (SiO_2) shell could moderate the toxicity to human skin dermal fibroblast neonatal (HDFn) cells.[7] Likewise PEGylation of ZnO NPs reduced their cytotoxicity to human immune cells.[8] Compared with the highly toxic pristine ZnO NPs, minimal cytotoxcity and genotoxicity of the NPs to human lymphoblastoid (WIL2-NS) cells was achieved by coating these particles with the components from supplemented cell culture medium. The coating in the above study was attained by soaking pristine ZnO NPs in supplemented cell culture medium consisting of RPMI 1640 medium, 5% Fetal bovine serum (FBS), 1% L-glutamine and 1% penicillin/streptomycin for 168 h at 4 ^{o}C, and the obtained NPs showed distinct adsorption of proteins on their surfaces.[9] However, the detailed structure of these pre-soaked NPs and the mechanism of their reduced toxicity are not fully understood or correlated.

For pristine ZnO NPs co-cultured with cells, one of the most significant interactions is *in-situ* formation of a NP-protein corona as a result of protein adsorption (from supplemented cell culture medium) onto the NP surface. The protein corona imparts a unique physicochemical character to NPs that consequently defines the biological identity of the particle.[10,11] It is believed that within the first seconds or minutes after immersion of NPs into cell culture medium containing serum, a soft corona is formed involving proteins with the highest mobility. Subsequently, the soft corona is replaced within hours by less mobile biomolecules that have a higher affinity for the NP surface (hard corona) due to the Vroman effect.[12] The normal cell culture duration (i.e. 24 h used in most cytotoxicity studies) is sufficiently long for the hard corona to develop.[13,14] The composition of the hard protein corona is very stable and as a result of its long residence time, the hard corona remains adsorbed to the NPs during biophysical events such as endocytosis[15] and is therefore more relevant for determining the physiological response of cells to NP exposure. It has been reported that the rapid formation of the hard corona within the cellular response time mitigates the toxicity of the original NP core.[16-18] However, in our previous study, pristine ZnO NPs with *in-situ*

[a] *Commonwealth Scientific and Industrial Research Organization (CSIRO), Manufacturing Flagship, Private Bag 33 Clayton, Victoria 3169, Australia*
[b] *ARC Centre of Excellence in Convergent Bio-Nano Science and Technology, Monash Institute of Pharmaceutical Sciences, Monash University, 381 Royal Parade, Parkville, VIC 3052, Australia*
[c] *CAS Key Laboratory of Biomedical Effects of Nanomaterials and Nanosafety, National Centre for Nanoscience and Technology, Beijing, China*
[d] *Department of Chemistry, Warwick University, Gibbet Hill, Coventry, CV4 7AL, United Kingdom*
† *These authors contributed equally to this work.*
Corresponding author e-mail: hong.yin@csiro.au

formed hard corona exhibited higher toxicity to WIL2-NS cells than NPs with a pre-coated protein layer.[9]

The composition of protein corona and its binding kinetics strongly depend on the physicochemical properties and concentration of the NPs.[19] Hence, the protein coating of NPs plays a primary role in determining the effective size, surface charge, and aggregation state of the newly formed bio-nanomaterials, influencing the biodistribution and triggering beneficial or adverse effects on the host system.[20,21] The protein structure varies when the surface functionalization of the NP is different. For example, native, amine ($-NH_2$) and carboxy (-COO-) modified SiO_2 NPs were examined following incubation in mammalian growth media containing FBS. The composition of the protein corona for each of the three types of NPs was unique, indicating a strong dependence of corona development on NP surface chemistry.[22] Such understanding hints the possibility that ZnO NPs with a pre-coated protein layer behave differently from pristine NPs in protein adsorption, thus rendering lower cytotoxicity.

In this paper, the cytotoxicity of pristine ZnO (uncoated) and ZnO NPs with pre-coated protein layer were investigated. The latter was prepared by incubating uncoated ZnO NPs in RPMI 1640 cell culture medium supplemented with 10% FBS at 37 ^{o}C under a humidified atmosphere with 5% CO_2 for 24 h, then isolated and dried. The production of reactive oxygen species (ROS) and dissolution of the two types of NPs were measured to understand their toxicological responses. The physicochemical variations between pre-coated and pristine ZnO NPs were studied in both dry state and in supplemented cell culture medium. The *in-situ* protein corona and pre-coated protein layer on the ZnO NPs were compared and their effects on cytotoxicity were discussed. To our knowledge, this is the first study on the continued evolution of hard protein corona in the supplemented cell culture medium.

Results

1. Cytotoxicity, NP dissolution and oxidative stress

Figure 1a shows the dependence of human hepatocellular carcinoma (HepG2) cell viability on NP concentration (0 -100 mg/L) in the presence of pristine and pre-coated ZnO NPs. For pristine ZnO NPs, the cell viability reduced significantly (from ~90% to ~20%) when particle concentration increased from 20 mg/L to 50 mg/L and further dropped to ~15% when the concentration increased to 100 mg/L. In contrast, the cell viability in the presence of pre-coated ZnO NPs remained high (85%-95%) within the whole range of tested NP concentrations (up to 100 mg/L). This suggests that pre-incubation of ZnO NPs in supplemented cell culture medium significantly mediated the toxicity of pristine NPs. This observation is consistent with our previous report that ZnO NPs coated with components from cell culture medium elicited low cytotoxicity to WIL2-NS cells.[9] To understand the mechanisms leading to the reduced toxicity of pre-coated ZnO, NP dissolution, cellular uptake and ROS generation, that are three key determinants of the toxicity paradigms of ZnO NPs were measured for both pristine and pre-coated ZnO NPs.

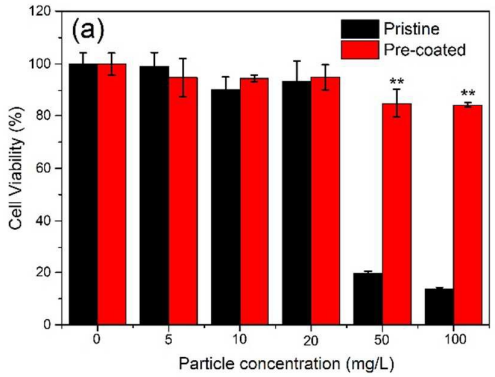

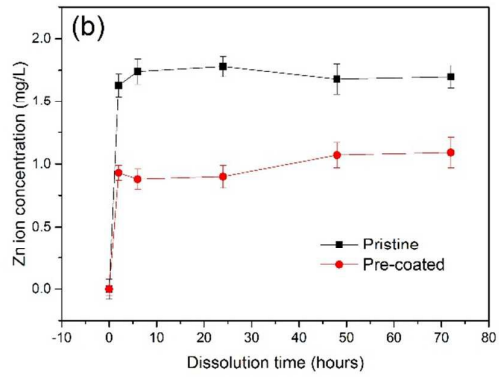

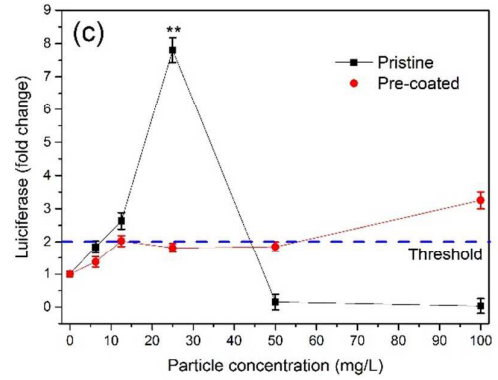

Figure 1. Cytotoxicity, dissolution and ROS generation ability of pristine and pre-coated ZnO NPs. (a) dependence of HepG2 cell viability on the NP concentration (0 -100 mg/L) after incubation with particles for 24 h; (b) dissolution kinetics (release of ionic Zn from ZnO NPs) in supplemented RPMI1640 cell culture medium at 37 ^{o}C; (c) ROS generation using HepG2-ARE stable cell line after incubation with NPs for 8 h. Two-folds of the untreated control luciferase signal were defined as the positive threshold in the test. A one-way analysis of variance following a post hoc least-significant difference multiple comparison test was used in the statistical analysis to comparing the two groups of the same treatment concentration. $^{**}P < 0.01$.

Figure 1b presents the dissolution kinetics (release of ionic Zn from ZnO particles) in supplemented RPMI1640 cell culture medium at 37 ^{o}C. Both pristine and pre-coated ZnO NPs exhibited similar dissolution profiles, i.e. a fast dissolution rate within the first 6 h followed by an equilibrium plateau. The equilibrium solubility of pre-coated ZnO NPs (0.9 mg/L, 1.8 wt %) is significantly lower than that of pristine ZnO NPs (1.7 mg/L, 3.4 wt %), suggesting that pre-coated particles had higher stability in supplemented RPMI1640 cell culture medium and released less Zn ions to the solution. The low weight percentage of dissolved species also implied that the majority of ZnO was present in the form of NPs. Different reports have shown that NPs exposed to cells in serum-free conditions can enter cells with higher efficiency than when they are covered by a corona in biological fluids.[13, 23] In our study, we used transmission electron microscopy (TEM) in an attempt to locate and quantify the numbers of particles in each cell. However, the contrast between ZnO particles and biological matrix is too low to enable identification. Recently, some new strategies involving synchrotron radiation analytical techniques have been developed to directly probe and quantify particles distributed throughout the cellular interior.[24, 25] The study on how to employ these new methods to our cellular system is on-going and beyond the scope of this paper.

Using antioxidant response element (ARE) reporter cells is one of the reliable and sensitive *in vitro* methodologies to measure the oxidative stress response in cell models based on the mechanism of mRNA transcription regulation by Nuclear-factor-E2-related factor (NRF2).[26, 27] According to our previous report, transcriptional level usually had a quick response from 4 h to 12 h and the signal peak was found at 8 h for NRF2 luciferase reporter test.[28] Therefore HepG2-ARE cell line was used to assess the ability of ROS production after exposure to NPs for 8 h. The correlation between luciferase activities (an indicator of oxidative stress and ROS level) and NP concentration is shown in Figure 1c. The oxidative stress induced by pristine NPs increased with the increase of NP concentration and reached a maximum when the NP concentration was 25 mg/L. At higher NP concentrations (50 mg/L and 100 mg/L), detected luciferase activities decreased significantly as a result of dramatic cell death (shown in Figure 1a). Comparatively, pre-coated ZnO NPs triggered modest luciferase activities up to 100 mg/L, suggesting no accumulation of intracellular ROS level within the range of tested NP concentrations. In order to reveal the possible reasons leading to variations in dissolution and ROS generation between pristine and pre-coated NPs, the characteristics of these two types of NPs were studied in the absence or presence of supplemented cell culture medium.

2.2 Pristine and pre-coated ZnO NPs in dry state

As presented in Figures 2a and b, TEM images of pristine ZnO NPs and pre-coated ZnO NPs suggest that both types of the NPs were mainly present in agglomerates. The specific surface area of pre-coated ZnO NPs (25.7 m^2/g) was very similar to that of pristine ZnO NPs (25.9 m^2/g), implying that their agglomeration states did not change due to the contact with cell culture medium. The pristine ZnO NPs (Figure 2a) were pseudo-spherical with an average size of 29 ± 10 nm. The enlarged image of a single particle shows its well defined surface (Figure 2a inset). For pre-coated NPs, surface coating was clearly visible (Figure 2b), although such coating was not uniform and appeared dependant on the curvature and local environment of the individual NPs. The Figure 2b inset shows a NP with a full coverage of surface coating and the thickness of the coating layer is about 5-8 nm. The nature of the surface coating acquired from cell culture medium and its interaction with the ZnO NPs were further identified using Fourier Transform Infrared (FTIR) spectroscopy (Figure 2c). For pristine ZnO NPs, only one specific absorbance peak was observed at 3430 cm^{-1} and this peak was attributed to surface hydroxyl groups (-OH). The spectrum of pre-coated ZnO NPs showed peaks at 1653 cm^{-1} and 1538 cm^{-1} that are distinct vibrational modes of amide I (C=O) and amide II (asymmetric stretch of COO^-), most likely due to surface-adsorbed amino acids from original RPMI1640 formulation or bovine serum albumin (BSA) from supplemented FBS. Based on the structure of -CO-NH- and the properties of hydroxyl groups on the ZnO surfaces, the interactions between adsorbed species (amino acids or BSA) and ZnO NPs are most likely mediated by hydrogen bonding and electrostatic forces. As reported by Yu et al.,[29] such interactions can result in a shift for the hydroxyl absorbance to a lower wave number in the FTIR spectrum. Indeed, as shown in Figure 2c, a shift was observed from 3430 cm^{-1} in the uncoated NPs to 3350 cm^{-1} in the pre-coated NPs. The thickness of the protein layer on the NPs is in agreement with the size of BSA, which is known to be ~ 6 nm.

To quantitatively determine the percentage of adsorbed species in the pre-coated ZnO NPs, thermal stability of pristine and pre-coated ZnO NPs was measured and the thermogravimetric analysis (TGA) results are shown in Figure 2d. Specifically, the pristine ZnO NPs were thermally stable upon the rise of temperature and negligible changes in mass were observed till 600 ^{o}C. In contrast, the weight of pre-coated ZnO NPs decreased with the increase of temperature and a total weight loss of 13% was observed in the heating process. There are two plausible stages of decomposition for pre-coated ZnO NPs. The first stage involved a weight loss due to evaporation of adsorbed water, about 5 wt % that ended around 150^{o}C. The second stage showed a sharp gradient resulting from loss of adsorbed proteins on particle surface, which was around 8 wt % of the total weight of the NPs.

The surface chemistry of pre-coated ZnO NPs was studied using XPS in comparison with that of pristine NPs. As shown in the survey spectra (Figure 3a), only Zn, O and C were detected in pristine ZnO particles, while a variety of components, including nitrogen (N), sodium (Na), calcium (Ca), and phosphorus (P) were detected on the surface of pre-coated NPs. The quantitative X-ray photoelectron spectroscopy (XPS) results (Table 1) indicate that the ratio of Zn to O is not stoichiometric with ~18% of oxygen deficiency. The amount of C is much less than that of Zn and O and could be due to adventitious carbon (a thin layer of carbonaceous material usually found on the surface of air exposed samples). For pre-coated ZnO NPs, the relative concentration of carbon increased significantly compared with Zn; the oxygen concentration also increased compared with that of pristine ZnO. Figures 3b and 3c show the XPS spectra of the C1s and N1s edges for pristine and pre-coated ZnO NPs, respectively. The carbon species of hydrocarbon (C-H: 285.0 eV), carbon bounded to nitrogen (C-N: 286.5 eV), amide carbon (N-C=O: 287.9 eV) and carbon bounded to oxygen (C=O: 290.0 eV) were distinct in pre-coated NPs. The N1s high resolution XPS spectrum also specifies the presence of C≡N and N-H characteristic protein functional groups at 399.9 eV.

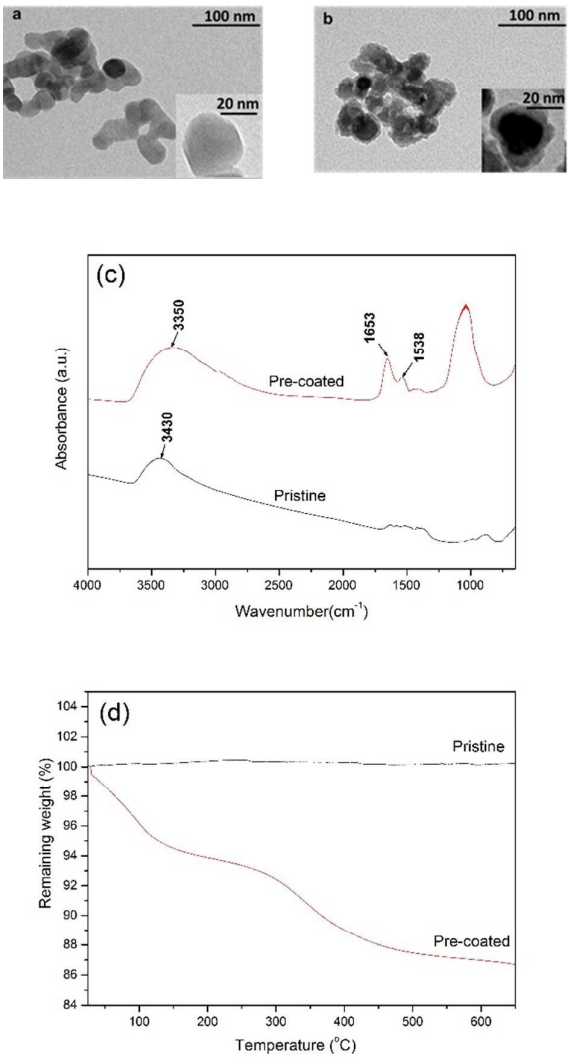

Figure 2. Characterization of pristine and pre-coated ZnO NPs in dry state. (a) TEM image of pristine ZnO NPs, where the inset shows a single particle with well-defined surfaces; (b) TEM image of pre-coated ZnO NPs. The inset shows a single particle with full coverage of surface coating; (c) FTIR spectra of pristine and pre-coated ZnO NPs; surface hydroxyl groups (-OH) were observed at 3430 cm^{-1} in pristine NPs. Pre-coated ZnO NPs show peaks of amide I (C=O) at 1653 cm^{-1} and amide II (asymmetric stretch of COO^-) at 1538 cm^{-1} due to surface-adsorbed amino acids or BSA. (d) TGA curves of the weights of pristine and pre-coated ZnO NPs versus increasing temperature. The pristine ZnO was thermally stable upon the rise of temperature while pre-coated ZnO NPs lost a total 13% of weight in the heating process.

Table 1 Quantitative XPS results showing atomic ratio of detected elements proportional to Zn in pristine and pre-coated NPs. ND: Not Detected.

Detected Element	Pristine NPs	Pre-coated NPs
Zn	1.00	1.00
O	0.82	1.68
C	0.34	1.36
N	ND	0.29
Na	ND	0.01
Ca	ND	0.03
P	ND	0.10

In summary, the above physicochemical characterisations of pre-coated ZnO NPs in dry state revealed formation of a hard protein corona during 24 h pre-incubation, which modified the surface of NPs. We also detected Ca, Na, K, and P on the surfaces of pre-coated ZnO NPs which were originated from the formulation of supplemented cell culture medium. This may indicate the development of an ion corona which decorated the protein layer and both of these ion and protein coronas could influence the cellular response to the NPs.[30]

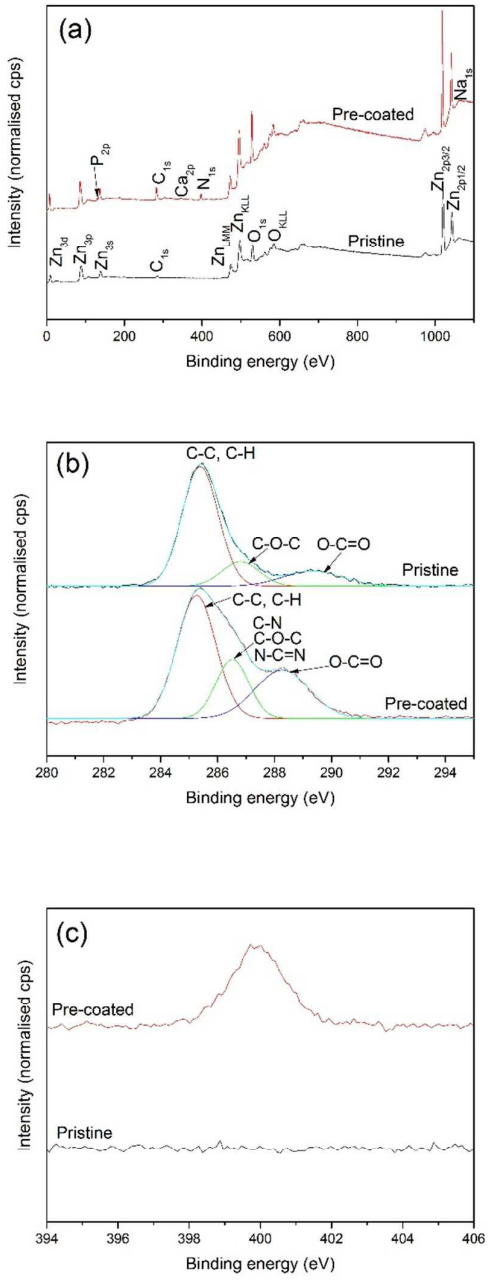

Figure 3. XPS spectra of pristine and pre-coated ZnO NPs: (a) survey (b) C1s edge, (c) N1s edge.

2.3 Pristine and pre-coated ZnO NPs dispersed in liquid

The surface charges and hydrodynamic sizes of the pristine and pre-coated ZnO NPs were measured in deionised water. The zeta potential of pristine ZnO NPs in water was +16.3 eV, consistent with the literature.[1] In contrast, the surface charge of pre-coated NPs dropped to -13.1 eV due to the adsorption of negatively charged species, such as BSA. The hydrodynamic size of pre-coated NPs (364 ± 22 nm) in water was slightly smaller than that of pristine ZnO NPs (409 ±73 nm). This could be caused by the presence of adsorption species that afforded a steric barrier for preventing NP agglomeration.

To quantitatively investigate the adsorbed biomolecule species and their affinity for the NP surfaces, sodium dodecyl sulfate polyacrylamide gel electrophoresis (SDS-PAGE) was used to analyse the gel of proteins from NPs and from the supernatant containing softly bound proteins. As shown in Figure 4a, there are two columns for each sample, the left one is the gel of the proteins from the supernatant and the right column is the gel of the proteins from the NPs. As expected, no proteins were detected in either the supernatant or pristine ZnO NPs which had no contact with any protein molecules. For pre-coated ZnO NPs, proteins were detected on the NPs but not in the supernatant, implying that no desorption was found during the washing process. This suggests that a hard protein corona was developed, which remained stable after the isolation and purification processes. Quantitatively, the relative amount of the proteins in the hard corona calculated by densitometry for the protein adsorbed on the NPs was shown in Figure 4b. The presence of proteins on the NPs was confirmed by gel electrophoresis of NPs with the 60 kDa band as the most abundant proteins adsorbed. This is because that both BSA (~ 67 kDa) and haemoglobin (~ 64 kDa) are major components of FBS. In Figure 4c, no desorption of protein was detected in the supernatant in the most abundant protein bands (~60 kDa). Above results indicated that proteins on the pre-coated NPs were stable and they were robust enough to maintain their affinity over an extended period of time in air during storage and in protein-free solution during the washing process.

2.4 Pristine and pre-coated ZnO NPs after co-cultured with supplemented cell culture medium for 24 h

In the process of cell culture, pristine and pre-coated ZnO NPs were co-cultured with cells in supplemented RPMI 1640 cell culture medium for 24 h, where they demonstrated significantly different cytotoxic behaviours to HepG2 ells. In this section, the evolution in the physicochemical properties of pristine and pre-coated NPs after interacting with supplemented cell culture medium for 24 h was studied in the absence of cells. Whenever possible, the NPs were analysed as their state in supplemented cell culture medium without further isolation and purification.

The surface charge of pristine NPs after incubated in supplemented medium for 24 h is negative (-11.8 eV) due to the formation of protein corona. And the surface charge of pre-coated NPs was very similar, at -11.2 eV. Figure 5 shows the morphologies of the NPs at 50 mg/L in supplemented cell culture medium after 24 h incubation. Both pristine and pre-coated NPs maintained as individual particles without agglomeration. The surfaces of pristine ZnO NPs were mottled and their edges were less well-defined (Figure 5a), and it is difficult to measure accurately the average sizes of the NPs. But in general, the average particle size was smaller than that in Figure 2a which is most likely due to limited ZnO dissolution. A close observation of single particles suggests the presence of cloud-like protein that adsorbed on the NP surfaces. The particle size and shape of pre-coated ZnO NPs after another 24 h incubation (Figure 5b) were very similar to those of pristine ZnO NPs (Figure 5a), but the outlines of the NPs were even more blurred. A higher magnification image showed a similar cloud-like protein corona on the NP surface. And overall, the NPs were covered by a protein layer, which may include previous protein coating during pre-incubation and newly formed protein corona.

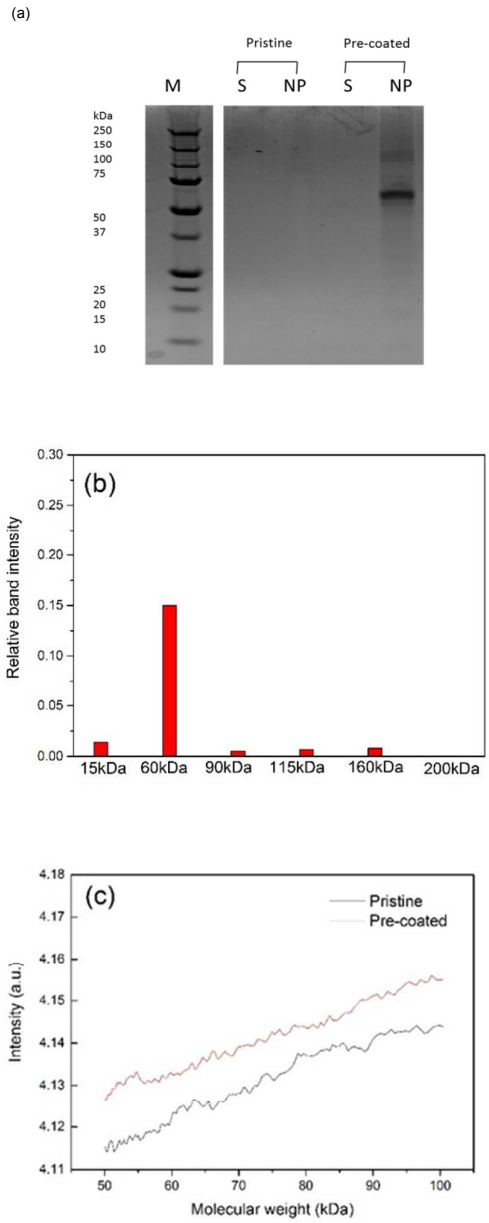

Figure 4. SDS-PAGE on adsorbed protein species and their affinity for ZnO NPs, (a) gel of proteins adsorbed on pristine and pre-incubated NPs (NP) and from supernatant (S) which contained softly bound proteins; (b) amount of proteins calculated by densitometry for the proteins adsorbed on pre-coated NPs; (c) amount of proteins detected in the supernatant in the most abundant protein bands (~60 kDa).

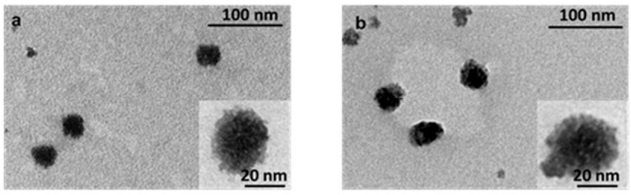

Figure 5. TEM images of ZnO NPs at 50 mg/L in supplemented cell culture medium after 24 h incubation without the presence of cells. (a) pristine ZnO NPs; (b) pre-coated ZnO NPs.

As indicated above, both pristine and pre-coated ZnO NPs developed protein coronas while interacting with supplemented medium during the cell culture process. The surface charge and morphology of the protein coronas developed are very similar, yet they elicit drastically different toxicities in HepG2 cells. To further investigate NP-protein interactions, the XPS spectra of pristine and pre-coated ZnO NPs after incubating in supplemented cell culture medium are presented in Figure 6 in survey and C1s edge, respectively. No obvious differences were identified between the two survey spectra, i.e., except for Zn, O, and C, both spectra designate the presence of N, P, Na, and Ca components from the cell culture medium. In Figure 6b, the intensity ratio of the peaks (C-N: 286.5 eV, N-C=O: 287.9 eV, C=O: 290.0 eV due to protein adsorption) to the hydrocarbon peak (C-H: 285.0 eV attributed to adventitious carbon) increased for the pre-coated NPs compared to the pristine NPs. This suggests that a large amount of proteins was detected in the pre-coated NPs.

Detailed examination on adsorbed proteins was performed using SDS-PAGE. Gels of proteins from pristine and pre-coated ZnO NPs (both incubated in supplemented cell culture medium for 24 h) were shown in Figure 7a. It is clear that some proteins were detected on pristine ZnO NPs after 24 h incubation and the protein profiles were very similar to that of pre-coated NPs. After the pre-coated NPs were incubated in supplemented cell culture medium for another 24 h, a significantly increased amount of proteins was detected in SDS gels (compared with Figure 4a) indicating that extra proteins adsorbed on the surface of pre-coated NPs. These results are consistent with the XPS observations. The relative amount of the proteins on NPs in the hard corona calculated by densitometry was shown in Figure 7b. Higher band intensities were recorded for almost all protein bands (15, 60, 90, 115, 160, 200 kDa) for the pre-coated ZnO NPs. Figure 7c shows the relative intensity of the protein band (60 kDa) of the supernatant obtained after washing. The amount of desorbed protein from pristine NPs was significantly higher than that from pre-coated NPs, indicating that more proteins were present as soft corona on the pristine NPs.

In summary, the amount of proteins adsorbed on pre-coated NPs was significantly higher and the affinity of proteins in supplemented culture medium for pre-coated NPs was stronger compared to that for pristine NPs. It has been reported that the adsorption of plasma proteins depends primarily on NP hydrophobicity and surface charge.[31] The surface charges of pristine NPs and pre-coated NPs after incubated in supplemented medium for 24 h were very similar (-11.8 eV and -11.2 eV, respectively). Nevertheless, pre-coated NPs trend to be more hydrophobic (due to the pre-existing protein layer) than pristine ZnO NPs with hydroxyl (–OH) as surface function groups (shown in Figure 2c).

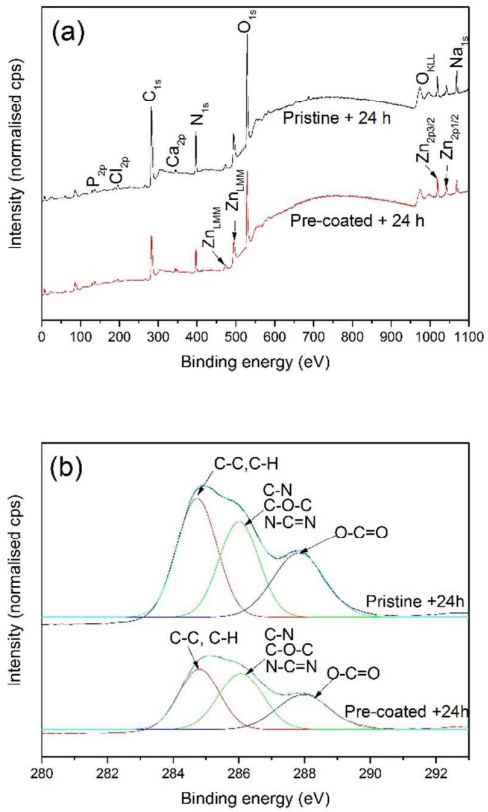

Figure 6. XPS spectra of pristine and pre-coated ZnO NPs after incubation in supplemented medium for 24 h: (a) survey, (b) C1s edge.

3. Discussion

Our study suggests that the cytotoxicities of pristine and pre-coated ZnO NPs were strongly dependent upon protein adsorption in supplemented cell culture medium. Similar to our findings, Hu et al. also demonstrated that the cytotoxicity of graphene oxide (GO) nanosheets was largely attenuated when GO was incubated with FBS due to the extremely high protein adsorption ability for the GO.[17] As production of ROS and particle dissolution are identified as two key determinants for the toxicity paradigms of ZnO, their correlations with protein adsorption on the two types of ZnO NPs are discussed below.

3.1 Protein adsorption and ROS generation.

In cellular mitochondria under normal conditions, ROS are generated at low levels and are neutralized by antioxidant enzymes such as glutathione (GSH). When exposed to excessive levels of ROS resulting in depletion of GSH and accumulation of oxidized glutathione (GSSG), e.g., under the conditions of oxidative stress, cells react by mounting further protective or injurious responses.[32]

(a)

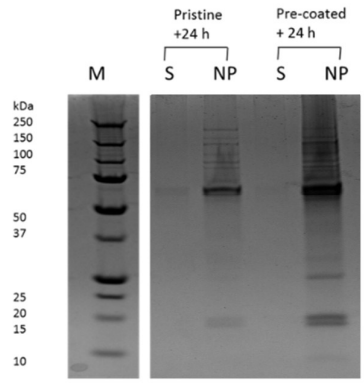

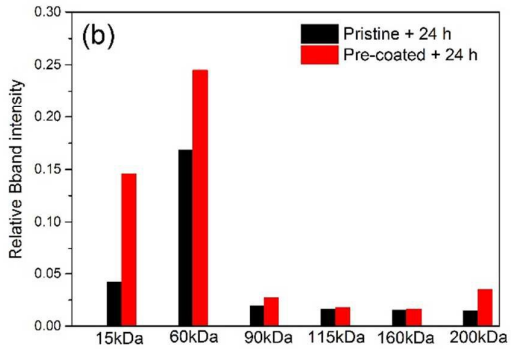

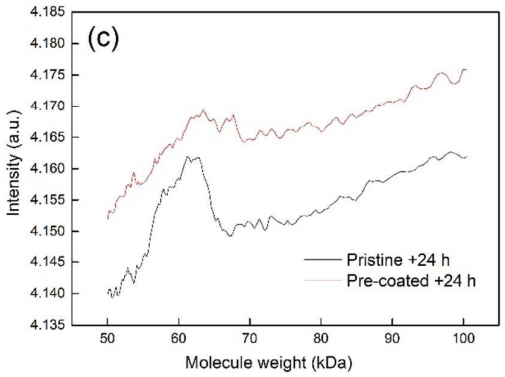

Figure 7. SDS-PAGE results on adsorbed protein species on pristine and pre-coated NPs after 24 hours incubating in supplemented cell culture medium, (a) the gel of proteins adsorbed on pristine and pre-incubated NPs (NP) and from supernatant (S); (b) the amount of proteins calculated by densitometry for proteins immobilised on the NPs; (c) The amount of proteins detected in supernatant in the most abundant protein bands (~60kDa).

In this study, significantly higher oxidative stress was detected when HepG2-ARE reporter cells were exposed to pristine ZnO NPs, which agrees well with our recent observation using Dichloro-dihydro-fluorescein diacetate (DCFH-DA) assay.[33] ZnO NPs are able to induce ROS resulting from their semiconductor properties. Unlike metals, which have a continuum of electronic states, the electrons in semiconductors possess energies only within certain bands. ZnO has a wide band gap (~3.3 eV), which corresponds to emission in the UV region. Consequently, UV light contains sufficient energy to promote electrons (e-) to the conduction band and create electron holes (h+) in the valence band. Electrons and holes often recombine quickly, but can also migrate to the NP surface where they react with adsorbed species.[34] As ZnO particle size decreases, more crystal defects are expected especially near the particle surface, which results in increased interstitial zinc and oxygen vacancies, and possibly a large number of valence band holes and/or conduction band electrons.[35] As demonstrated by our XPS data, distinct oxygen deficiency found in pristine ZnO NPs was very likely to be related to these crystal defects. The electron-hole pairs are available to serve in redox reactions even in the absence of UV light.[36] For example, electrons are good reducers and can move to the particle surface to react with dissolved oxygen molecules to generate superoxide radical anions ($\bullet O^{2-}$), which in turn react with H^+ to generate ($HO_2\bullet$) radicals. These $HO_2\bullet$ molecules then produce hydrogen peroxide anions (HO^{2-}) following a subsequent encounter with electrons.[37, 38] Hydrogen peroxide anions can then react with hydrogen ions to produce hydrogen peroxide (H_2O_2) and other ROS molecules in cellular environments.[39, 40] These ROS can trigger redox-cycling cascades in the cell, or on adjacent cell membranes, leading to depletion of endogenous cellular reserves of antioxidants so that irreparable oxidative damage to cells occurs.[41]

The pristine ZnO NPs were positively charged. FBS has a number of protein and amino acid components, with BSA being the most abundant. BSA is overall negatively charged and therefore easily bound to ZnO NPs through electrostatic interactions. The adsorption of proteins effectively shielded the ZnO surfaces and blocked the transferring of ROS molecules to cellular components, thus reducing intracellular oxidative stress. Our findings are consistent with the observations reported by Casals et al. in which the production of ROS was decreased in monocytic cell line (THP-1) cells when cobalt oxide NPs were incubated with serum for 48 h.[42]

Both pristine and pre-coated ZnO developed protein layers after incubated in supplemented cell culture medium and the types of the adsorbed proteins detected using SDS-PAGE were largely the same, with BSA being the most abundant. However, the quantities of proteins on pre-coated NPs were significantly larger than those detected on the pristine NPs. The pre-coated ZnO NPs have an existing stable hard protein corona, and its presence increased further adsorption of proteins during the cell culture process. While for the pristine ZnO NPs, some adsorbed proteins were loosely bound to NP surface (soft corona) and were easily washed off. The elevated protein adsorption in the form of strongly bound hard corona on pre-coated ZnO NPs is likely to be a cause for their lower ROS generation compared with the pristine NPs.

The protein corona consists of proteins and other biomolecules, which adsorb onto the NPs to reduce their surface energy, thereby rendering a new complex unit interacting with cells. The interaction between NPs and proteins also induces conformational changes to the adsorbed proteins. The NP surface can also introduce thermal instability to the adsorbed protein molecules, making them susceptible to chemical denaturation.[43] ZnO NPs induced unfolding of the periplasmic domain of the ToxR protein of Vibrio cholera, rendering the protein prone to denaturation by chaotropic agents.[44] Interestingly, ZnO NPs were able to stabilize the α-helical content of lysozyme against denaturing agents.[45] The structure of plasma proteins after binding on ZnO NP surface requires more detailed examination but is beyond the scope of this study.

3.2 Protein adsorption and ZnO dissolution

The dependence of Zn ion release from NPs in Figure 1b suggests that pre-adsorbed proteins also enhance the stability of NPs. This observation agrees well with Kittler et al.'s study using polyvinylpyrrolidone-stabilized Ag NPs, in which the formation of Ag-protein coronas with BSA and fetal calf serum reduced the cytotoxicity of human mesenchymal stem cells (hMSCs) by inhibiting the release of free Ag ions from the NPs.[46] The equilibrium solubility of pristine ZnO NPs (1.7 mg/L, about 26 μM) is much lower than the toxic level of Zn ions (100 μM) [47], suggesting that extracellular ZnO dissolution may not be an influential factor of the observed cytotoxicity for pristine ZnO. Several studies on ZnO NPs demonstrated that intracellular dissolution after NPs were internalized by cells would be more significant. Muller et al reported that ZnO nanowires were comparatively stable at extracellular pH, whereas they dissolved very rapidly in a simulated body fluid of lysosomal pH (pH=4.5).[48] Shen et al. also demonstrated a strong correlation between ZnO NP–induced cytotoxicity and free intracellular zinc concentration (R^2 = 0.945) in human immune cells.[49] Reduced toxicity in the rodent lung and zebrafish embryos were achieved by doping ZnO NPs with iron, which distinctly enhanced stability and decreased solubility of undoped ZnO NPs.[50] Therefore, the higher stability of pre-coated ZnO NPs shown in Figure 1b could be closely related to its lower cytotoxicity.

Protein corona forms immediately after NPs are introduced to the cell culture medium. In the presence of a protein layer bound tightly on pre-coated ZnO NP surfaces, zinc ions that released from ZnO NPs are trapped by the corona due to their mutual electrostatic attraction with the protein. The dissolution equilibrium of this complex therefore was stalled as the local zinc ion concentration within the corona was high and stable, unlike the situation when zinc ions are released by pristine NPs and then diluted by the vast volume of solvent without the presence of the corona. In addition to this, as aforementioned, released zinc ions could also play an essential role in protein tertiary structure, such as zinc fingers.[51] In other words zinc ions could integrate with serum albumin and other proteins to stabilize or alter their structures. With the presence of more proteins on pre-coated NPs, the likelihood for released Zn ions to be involved in above Zn ions-protein interaction is also higher, thus reducing the level of detected Zn ions in solution and further impacting cytotoxicity.

4. Conclusions

We studied the effects of continued evolution and transformation of protein corona on the cytotoxicity of ZnO NPs. Our results revealed that the pre-existing protein layer on ZnO NPs (obtained by pre-incubating pristine ZnO NPs in supplemented cell culture medium) facilitated further protein adsorption during the cell culture process. The formation of the corona with more proteins and strong affinity for the pre-coated NPs enhances ZnO stability and inhibits ROS generation, leading to reduced cytotoxicity compared with pristine ZnO NPs. Reducing the cytotoxicity of ZnO and other types of engineered NPs by such pre-formed protein layer provides an alternative and convenient way to engineering nanomaterials for safe biomedical and environmental applications.

5. Experimental

5.1 Materials

The precursors used for ZnO NPs synthesis were purchased from Sigma-Aldrich. Biological reagents used for the experiments with cells, such as RPMI 1640 medium, FBS were purchased from Gibco Life Technologies. L-glutamine (200 mM), penicillin/streptomycin (with 10,000 units penicillin and 10mg streptomycin/ml), Phosphate-Buffered Saline (PBS, pH=7.4 biotechnology performance certified), were purchased from Sigma–Aldrich.

5.2 NPs preparation

Pristine ZnO NPs: ZnO NPs are prepared using a proprietary process developed by the CSIRO Materials Science and Engineering (Melbourne, Australia). Interested readers may contact the corresponding author to discuss the supply of these ZnO NPs for academic research.

Pre-coated ZnO NPs: Pristine ZnO NPs (3 g) were incubated in supplemented cell culture medium consisting of RPMI 1640 medium, 10 % FBS, 1% L-glutamine and 1% penicillin/streptomycin at 37 ^{o}C under a humidified atmosphere with 5% CO_2 for 24 h. Then NPs were then separated from supplemented cell culture medium by centrifuging at 10,000 rpm for 10 min and dried under vacuum overnight at room temperature.

5.3 Cell culture, cell viability and oxidative stress tests

HepG2 cells and their derivative ARE reporter cells (HepG2-ARE) were cultured at 37 ^{o}C in a 5% CO_2 atmosphere in RPMI 1640 medium supplemented with 10% FBS. HepG2-ARE was constructed from Cignal Lenti ARE reporter assay kit (SABiosciences, Frederick, MD, USA) and maintained after cellular monoclonal process. This cell line was used to assess the ability of ROS production induced by extrinsic toxicants as previously described.[28] All cells were seeded at a density of 5×10^3 cells per well in a 96-well plate supplemented medium and incubated for 24 h. The medium was then replaced with 100 μL of medium containing various equivalent concentrations of NPs. After co-cultured with NPs for 24 h, cytotoxicity was measured using CCK-8 Kits (Dojindo Molecular Technologies, Tokyo, Japan) according to the manufacturer's protocol. The absorbance was measured at 450 nm with a reference at 600 nm using Infinite M200 microplate reader (Tecan, Durham). In oxidative stress test, HepG2-ARE cells were exposed to NPs for 8 h, then lysed in 100 mL 1× passive lysis buffer (Promega, USA). Luciferase assays were carried out with 50 μL lysate using the luciferase reporter assay system (E1501 kit, Promega, USA) in a chemiluminescence analyzer with automatic injector system Infinite M200 microplate reader (Tecan, Durham, USA). Luciferase activities (response signal of oxidative stress) were expressed as fold induction relative to values obtained from untreated control cells. The cellular viability and oxidative stress results represented the mean of at least three independent experiments, each carried out in duplicate.

5.4 Dissolution of ZnO particles

The solubility of the ZnO NPs was measured in the supplemented cell culture medium without the presence of cells. Specifically, ZnO NPs (5 mg) were put into 100 mL of supplemented RPMI 1640 cell culture medium in a plastic tube and the resulting ZnO concentration was 50 mg/L. The plastic tube was placed in a water bath shaker maintained at 37 ^{o}C. At each time interval (0 h, 2 h, 6 h, 24 h, 48 h and 120 h), a 1.5 mL aliquot was taken out from the suspension and centrifuged at 10,000 rpm for 30 min; 1 mL of the

supernatant was added to 9 mL of supplemented RPMI 1640 cell culture medium, and the resulting zinc solution was digested and followed by elemental analysis using Inductively Coupled Plasma-Atomic Emission Spectroscopy (Varian 730 Axial ICP-AES) to determine the Zn concentration.

5.5 Physico-chemical characterizations

5.5.1 NPs in dry state

A few milligrams of the ZnO NPs were dispersed in deionised water and briefly sonicated or 10 min (Branson 3510, 100W, 42 kHz) to form a colloidal dispersion. Carbon-coated grids (copper, 300 mesh) were glow discharged in nitrogen for 30 s to render them hydrophilic. 5 µL of the dispersion was applied to the freshly-prepared grids. After 2 min, excess dispersion was wicked off using filter paper (Whatman 541) and the grids were dried in air for 15 min. The morphologies of the NPs were studied using Transmission Electron Microscope (TEM, JEOL, 100CX-II, Japan). The specific surface areas of NPs were determined by the Brunauer-Emmett-Teller (BET) using a Micromeritics Tristar II 3020 instrument. Interactions between protein coatings and surfaces of the ZnO NPs were investigated by Fourier Transform Infrared (FTIR) spectroscopy using a PerkinElmer FTIR 2000. The thermal stability of pre-coated ZnO NPs was studied using a Setaram Setsys Evolution 1750 Thermal Analysis system. The surface chemistry of pristine and pre-coated ZnO NPs was quantitatively determined by X-ray photoelectron spectroscopy (XPS). Specifically, powdered ZnO samples were placed in individual wells of a sample holder and were irradiated with X-rays under ultra-high vacuum using a Kratos HS spectrometer, fitted with a monochromated Al Kα source. Wide scan survey spectra were recorded to identify and quantify all elements present on the NP surfaces then fine scans on the C and N edges were performed.

5.5.2 NPs dispersed in liquid

The z-average hydrodynamic diameter of the ZnO NPs in deionised water (Milli-Q, 18.2 MΩ cm) was obtained by Dynamic Light Scattering (DLS) using a Malvern Zetasizer Nano Z system. Reference standards (Duke polystyrene latex with a nominal diameter of 100 nm, and NIST RM8013 gold nanoparticles with a nominal diameter of 60 nm) were used to verify the performance of the instrument. Electrophoretic-mobility measurement of zeta potential (surface charge) in deionised water was also performed using the Malvern Zetasizer Nano Z system.

5.5.3 NPs after co-cultured with supplemented cell culture medium for 24 h

Whenever possible, the interested physicochemical characteristics were studied from the state in supplemented cell culture medium without further isolation and purification. For example, TEM samples were prepared directly from a dispersion containing 50 mg/L ZnO NPs in supplemented cell culture medium. The dispersion was ultrasonicated for 10 min (Branson 3510, 100W, 42 kHz) and then a droplet of the suspension was taken off and dropped onto TEM grids. For the XPS study, one drop of ZnO dispersion (50 mg/L) in supplemented cell culture medium was placed onto individual well of a sample holder and allowed to dry overnight. The process was repeated twice to ensure a dense coverage of the NPs. The survey spectra and fine spectra were then collected on the dried samples.

5.6 SDS-PAGE

Pristine and pre-coated ZnO NPs were dispersed in PBS to a concentration of 50 mg/L. After ultrasonication (Branson 3510, 100W, 42 kHz) for 10 min, a uniform dispersion was attained and then centrifuged at 10,000 rpm for 10 min to pellet out the NPs. To wash off the organic species softly bound to the NP surfaces, the pellet was further washed twice using PBS and centrifuged. Immediately after the last centrifugation, the pellet and supernatant (collected after each centrifuge) were respectively re-suspended in protein loading buffer [62.5mM Tris-HCL pH=6.8, 2% (w/v) SDS, 10% glycerol, 0.04MDTT and 0.01% (w/v) bromophenol blue], it was then boiled for 5 min at 100 ^{o}C and equal sample volumes were loaded in 12% gel polyacrylamide gel. Gel electrophoresis was performed at 120 V, 400 mA for about 60 min, until the protein neared the end of the gel. The gels were stained for 1 h in coomassie blue staining [50% methanol, 10% acetic acid, 2.5% (w/v) brilliant blue] and destrained overnight in [50% methanol, 10% acetic acid]. Gels were scanned using a Bio-Rad GS-800 calibrated densitometer scanner and gel densitometry was performed using image J.

5.7 Statistical Analysis

The data were expressed as mean ± standard deviation (mean±SD). All the statistical analyses were implemented using SPSS v19.0 (SPSS Inc., Chicago, USA). A one-way analysis of variance following a post hoc least-significant difference multiple comparison test was used to compare the uncoated and pre-coated ZnO NPs in the study. Mean differences with P <0.05 were considered significant.

Acknowledgements

This work was funded by the CSIRO Manufacturing Flagship, the CSIRO Advanced Materials Transformational Capabilities Platform, the National Natural Science Foundation of China (21477029 and 21277080) and the Chinese Academy of Sciences (XDA09040400). The authors would like to thank Ms. Lynne Waddington, Dr. Thomas Gengenbach and Dr Yong Peng, from CSIRO for their characterisation work using TEM, XPS, and SDS-PAGE respectively.

References

1 H. Yin, V. A. Coleman, P. S. Casey, B. Angel, H. J. Catchpoole, L. Waddington and M. J. McCall, *J. Nanopart. Res.*, 2015, **17**, 1-19.
2 V. Sharma, R. K. Shukla, N. Saxena, D. Parmar, M. Das and A. Dhawan, *Toxicol. Lett.*, 2009, **185**, 211-218.
3 Z. Huang, X. Zheng, D. Yan, G. Yin, X. Liao, Y. Kang, Y. Yao, D. Huang and B. Hao, *Langmuir*, 2008, **24**, 4140-4144.
4 X. Zhu, L. Zhu, Z. Duan, R. Qi, Y. Li and Y. Lang, *J. Environ. Sci. Heal. A Tox. Hazard. Subst. Environ. Eng.*, 2008, **43**, 278-284.
5 B. Wang, W. Feng, M. Wang, T. Wang, Y. Gu, M. Zhu, H. Ouyang, J. Shi, F. Zhang, Y. Zhao, Z. Chai, H. Wang and J. Wang, *J. Nanopart. Res.*, 2008, **10**, 263-276.
6 X. Hu, S. Cook, P. Wang and H.-m. Hwang, *Sci. Total Environ.*, 2009, **407**, 3070-3072.
7 M. Ramasamy, M. Das, S. S. An and D. K. Yi, *Int. J. Nanomed.*, 2014, **9**, 3707-3718.

8 M. Luo, C. Shen, B. N. Feltis, L. L. Martin, A. E. Hughes, P. F. Wright and T. W. Turney, *Nanoscale*, 2014, **6**, 5791-5798.
9 H. Yin, P. S. Casey, M. J. McCall and M. Fenech, *Langmuir*, 2010, **26**, 15399-15408.
10 J. Wolfram, Y. Yang, J. Shen, A. Moten, C. Chen, H. Shen, M. Ferrari and Y. Zhao, *Colloids Surf. B Biointerfaces*, 2014, **124**, 17-24.
11 C. D. Walkey and W. C. Chan, *Chem. Soc. Rev.*, 2012, **41**, 2780-2799.
12 T. Cedervall, I. Lynch, S. Lindman, T. Berggard, E. Thulin, H. Nilsson, K. A. Dawson and S. Linse, *Proc. Natl. Acad. Sci. USA*, 2007, **104**, 2050-2055.
13 A. Lesniak, F. Fenaroli, M. P. Monopoli, C. Aberg, K. A. Dawson and A. Salvati, *ACS Nano*, 2012, **6**, 5845-5857.
14 C. Ge, J. Du, L. Zhao, L. Wang, Y. Liu, D. Li, Y. Yang, R. Zhou, Y. Zhao, Z. Chai and C. Chen, *Proc. Natl. Acad. Sci. USA*, 2011, **108**, 16968-16973.
15 M. P. Monopoli, D. Walczyk, A. Campbell, G. Elia, I. Lynch, F. B. Bombelli and K. A. Dawson, *J. Am. Chem. Soc.*, 2011, **133**, 2525-2534.
16 J. Shi, H. L. Karlsson, K. Johansson, V. Gogvadze, L. Xiao, J. Li, T. Burks, A. Garcia-Bennett, A. Uheida, M. Muhammed, S. Mathur, R. Morgenstern, V. E. Kagan and B. Fadeel, *ACS Nano*, 2012, **6**, 1925-1938.
17 W. Hu, C. Peng, M. Lv, X. Li, Y. Zhang, N. Chen, C. Fan and Q. Huang, *ACS Nano*, 2011, **5**, 3693-3700.
18 H., N. Saito, Y. Matsuda, Y. A. Kim, K. C. Park, T. Tsukahara, Y. Usui, K. Aoki, M. Shimizu, N. Ogihara, K. Hara, S. Takanashi, M. Okamoto, N. Ishigaki, K. Nakamura and H. Kato, *Int. J. Nanomed.*, 2011, **6**, 3295-3307.
19 P. Rivera Gil, G. Oberdorster, A. Elder, V. Puntes and W. J. Parak, *ACS Nano*, 2010, **4**, 5527-5531.
20 L. Wang, J. Li, J. Pan, X. Jiang, Y. Ji, Y. Li, Y. Qu, Y. Zhao, X. Wu and C. Chen, *J. Am. Chem. Soc.*, 2013, **135**, 17359-17368.
21 A. E. Nel, L. Madler, D. Velegol, T. Xia, E. M. Hoek, P. Somasundaran, F. Klaessig, V. Castranova and M. Thompson, *Nat. Mater.*, 2009, **8**, 543-557.
22 N. P. Mortensen, G. B. Hurst, W. Wang, C. M. Foster, P. D. Nallathamby and S. T. Retterer, *Nanoscale*, 2013, **5**, 6372-6380.
23 S. Ritz, S. Schottler, N. Kotman, G. Baier, A. Musyanovych, J. Kuharev, K. Landfester, H. Schild, O. Jahn, S. Tenzer and V. Mailander, *Biomacromolecules*, 2015, **16**, 1311-1321.
24 L. Wang, T. Zhang, P. Li, W. Huang, J. Tang, P. Wang, J. Liu, Q. Yuan, R. Bai, B. Li, K. Zhang, Y. Zhao and C. Chen, *ACS nano*, 2015, **9**, 6532-6547.
25 S. A. James, B. N. Feltis, M. D. de Jonge, M. Sridhar, J. A. Kimpton, M. Altissimo, S. Mayo, C. Zheng, A. Hastings, D. L. Howard, D. J. Paterson, P. F. Wright, G. F. Moorhead, T. W. Turney and J. Fu, *ACS nano*, 2013, **7**, 10621-10635.
26 R. Y. Prasad, J. K. McGee, M. G. Killius, D. A. Suarez, C. F. Blackman, D. M. DeMarini and S. O. Simmons, *Toxicol. In Vitro*, 2013, **27**, 2013-2021.
27 K. W. Kang, S. J. Lee and S. G. Kim, *Antioxid. Redox Sign.*, 2005, **7**, 1664-1673.
28 R. Chen, X. Shi, R. Bai, W. Rang, L. Huo, L. Zhao, D. Long, Y. P. David and C. Chen, *Aerosol Air Qual. Res.*, 2015, **15**, 284-294.
29 C. H. Yu, A. Al-Saadi, S.-J. Shih, L. Qiu, K. Y. Tam and S. C. Tsang, *J. Phys. Chem. C*, 2009, **113**, 537-543.
30 M. Xu, J. Li, H. Iwai, Q. Mei, D. Fujita, H. Su, H. Chen and N. Hanagata, *Sci. Rep.*, 2012, **2**, 406.
31 P. Aggarwal, J. B. Hall, C. B. McLeland, M. A. Dobrovolskaia and S. E. McNeil, *Adv. Drug Deliv. Rev.*, 2009, **61**, 428-437.
32 G. G. Xiao, M. Wang, N. Li, J. A. Loo and A. E. Nel, *J. Biol. Chem.*, 2003, **278**, 50781-50790.
33 R. Chen, L. Huo, X. Shi, R. Bai, Z. Zhang, Y. Zhao, Y. Chang and C. Chen, *ACS Nano*, 2014, **8**, 2562-2574.
34 G.-D. Fang, D.-M. Zhou and D. D. Dionysiou, *J. Hazard. Mater.*, 2013, **250–251**, 68-75.
35 S. K. Sharma, P. K. Pujari, K. Sudarshan, D. Dutta, M. Mahapatra, S. V. Godbole, O. D. Jayakumar and A. K. Tyagi, *Solid State Commun.*, 2009, **149**, 550-554.
36 H. Yang, C. Liu, D. Yang, H. Zhang and Z. Xi, *J. Appl. Toxicol.*, 2009, **29**, 69-78.
37 I. A. Salem, *Monatsh. Chem.*, 2000, **131**, 1139-1150.
38 N. Padmavathy and R. Vijayaraghavan, *Sci. Technol. Adv. Mat.*, 2008, **9**, 035004.
39 A. J. Hoffman, E. R. Carraway and M. R. Hoffmann, *Environ. Sci. Technol.*, 1994, **28**, 776-785.
40 H. Yin and P. S. Casey, *RSC Adv.*, 2014, **4**, 26149-26157.
41 J. W. Rasmussen, E. Martinez, P. Louka and D. G. Wingett, *Expert Opin. Drug Deliv.*, 2010, **7**, 1063-1077.
42 E. Casals, T. Pfaller, A. Duschl, G. J. Oostingh and V. F. Puntes, *Small*, 2011, **7**, 3479-3486.
43 S. R. Saptarshi, A. Duschl and A. L. Lopata, *J. Nanobiotechnol.*, 2013, **11**, 26.
44 T. Chatterjee, S. Chakraborti, P. Joshi, S. P. Singh, V. Gupta and P. Chakrabarti, *Febs J.*, 2010, **277**, 4184-4194.
45 S. Chakraborti, T. Chatterjee, P. Joshi, A. Poddar, B. Bhattacharyya, S. P. Singh, V. Gupta and P. Chakrabarti, *Langmuir*, 2010, **26**, 3506-3513.
46 S. Kittler, C. Greulich, J. Diendorf, M. Köller and M. Epple, *Chem. Mater.*, 2010, **22**, 4548-4554.
47 W. S. Lin, Y. Xu, C. C. Huang, Y. F. Ma, K. B. Shannon, D. R. Chen, Y. W. Huang, *J. Nanopart. Res.* 2009, **11**, 25-39.
48 K. H. Muller, J. Kulkarni, M. Motskin, A. Goode, P. Winship, J. N. Skepper, M. P. Ryan and A. E. Porter, *ACS nano*, 2010, **4**, 6767-6779.
49 C. Shen, S. A. James, M. D. de Jonge, T. W. Turney, P. F. Wright and B. N. Feltis, *Toxicol. Sci.*, 2013, **136**, 120-130.
50 T. Xia, Y. Zhao, T. Sager, S. George, S. Pokhrel, N. Li, D. Schoenfeld, H. Meng, S. Lin, X. Wang, M. Wang, Z. Ji, J. I. Zink, L. Madler, V. Castranova, S. Lin and A. E. Nel, *ACS nano*, 2011, **5**, 1223-1235.
51 M. J. Osmond-McLeod, R. I. Osmond, Y. Oytam, M. J. McCall, B. Feltis, A. Mackay-Sim, S. A. Wood and A. L. Cook, *Part. Fibre. Toxicol.*, 2013, **10**, 54.